



Cite this: DOI: 10.1039/d6sc01625a

All publication charges for this article have been paid for by the Royal Society of Chemistry

# <sup>18</sup>F-labelling of (hetero)aryl halides *via* sequential Miyaura borylation/copper-mediated radiofluorination

Abdias N. Noel,<sup>a</sup> Samuel G. Greco,<sup>a</sup> Mami Horikawa,<sup>a</sup> Taylor E. Spiller,<sup>a</sup> Diana L. Nichols,<sup>a</sup> Jason A. Witek,<sup>b</sup> Allen F. Brooks,<sup>b</sup> Peter J. H. Scott<sup>\*a</sup> and Melanie S. Sanford<sup>†a</sup>

This article describes the development of a mild, general, and highly reproducible method for the radiofluorination of (hetero)aryl iodide, bromide, and chloride substrates. This transformation proceeds *via* sequential Pd-catalysed Miyaura borylation with B<sub>2</sub>Pin<sub>2</sub> followed by *in situ* Cu-mediated radiofluorination of the (hetero)aryl-BPin intermediate with K<sup>18</sup>F. Successful implementation of this method required identifying and replacing/removing components of the borylation reaction that impede the radiofluorination step. This method is applied to electronically and sterically diverse (hetero)aryl halides and enables the synthesis of <sup>18</sup>F-labelled analogues of bioactive molecules such as indomethacin, dimethomorph, and metaxalone. In addition, this sequence is effective for the radiofluorination of a variety of amino acids and peptides.

Received 25th February 2026

Accepted 30th April 2026

DOI: 10.1039/d6sc01625a

rsc.li/chemical-science

## Introduction

Fluorine-18 is the most common radionuclide used in positron emission tomography (PET) imaging, based on its attractive half-life ( $t_{1/2} \sim 110$  min) and favorable imaging properties.<sup>1</sup> More than 60% of FDA-approved radiotracers for PET imaging contain a C–<sup>18</sup>F bond, and among these 25% are (hetero)aryl fluorides (Ar<sup>18</sup>F).<sup>2</sup> As the applications of nuclear medicine in drug discovery, diagnostic imaging, and disease therapy<sup>3–5</sup> expand, the demand for new and increasingly complex <sup>18</sup>F-labelled (hetero)aromatic molecules continues to accelerate.<sup>6</sup>

Over the past decade, the copper-mediated radiofluorination (CMRF) of (hetero)aryl boron compounds [ArB(OR)<sub>2</sub>] has emerged as a versatile method for late-stage construction of Ar–<sup>18</sup>F bonds.<sup>7</sup> These transformations are particularly powerful in the context of electron-neutral and electron-rich (hetero)arene scaffolds, where traditional nucleophilic aromatic substitution (S<sub>N</sub>Ar)<sup>8</sup> reactions fail. CMRF was developed independently by our team<sup>9,10</sup> and by Gouverneur and coworkers.<sup>11</sup> It has since been expanded by other groups<sup>12,13</sup> and applied to the synthesis of numerous radiotracers, including [<sup>18</sup>F]F-DOPA,<sup>14</sup> [<sup>18</sup>F]flumazenil,<sup>15</sup> and [<sup>18</sup>F]TRACK.<sup>16</sup> Despite this progress, there are challenges that limit even wider application and clinical translation of CMRF. First, preparing the requisite ArB(OR)<sub>2</sub> precursors in high yield and purity remains a bottleneck. While

a variety of synthetic methods are available for C(sp<sup>2</sup>)–B bond formation,<sup>17</sup> many of these afford poor yields with densely functionalized pharmaceutical candidates and/or peptides. Second, even when borylation is successful, the isolation and purification of structurally complex ArB(OR)<sub>2</sub> is often challenging. Finally, once isolated, many of the ArB(OR)<sub>2</sub> products have limited shelf-stability due to degradation *via* hydrolysis and/or protodeboronation.<sup>14,18,19</sup> This can detrimentally impact the radiolabeling yield, tracer purification, and reproducibility, all of which are critical for clinical applications.<sup>14,18</sup>

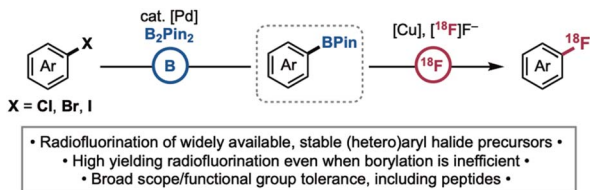
We sought to address these challenges by developing sequences that generate ArB(OR)<sub>2</sub> *in situ* from stable, readily available, and inexpensive starting materials. These ArB(OR)<sub>2</sub> intermediates could then be telescoped directly to CMRF without the need to isolate, purify, or store sensitive organoboron species. We recently demonstrated proof-of-concept for this approach in a tandem Ir-catalysed C–H borylation/CMRF reaction.<sup>20</sup> This method leverages abundant and stable arene precursors and enables the late-stage C–H radiofluorination of a range of substrates. However, the sequence is limited by the often-poor site selectivity of C–H borylation with complex bioactive scaffolds. It also exhibits moderate functional group compatibility and suffers from reproducibility issues, with standard deviations in radiochemical yields of up to 20%. Overall, a selective, general, mild, and reproducible alternative would be highly enabling for the radiofluorination of bioactive scaffolds, including amino acids and peptides.

This article describes a borylation/radiofluorination sequence that starts from abundant, readily available, and stable (hetero)aryl halides (Scheme 1). Currently, the direct

<sup>a</sup>Department of Chemistry, University of Michigan, 930 North University Avenue, Ann Arbor, Michigan, 48109, USA. E-mail: mssanford@umich.edu

<sup>b</sup>Department of Radiology, University of Michigan, 1301 Catherine, Ann Arbor, Michigan, 48109, USA. E-mail: pjhscott@umich.edu





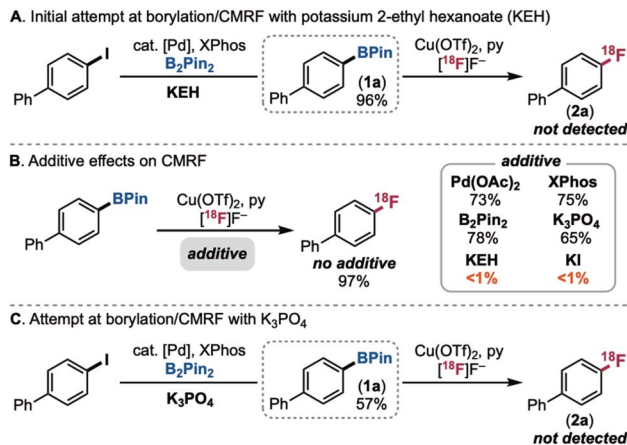
Scheme 1 This work:  $^{18}\text{F}$ -fluorination of (hetero)aryl halides via sequential Miyaura borylation/copper-mediated radiofluorination.

radiofluorination of aryl halides (particularly electron neutral or -rich derivatives that are not reactive in traditional  $\text{S}_{\text{N}}\text{Ar}$  pathways) remains challenging. The few known examples exhibit modest scope and functional group compatibility and/or afford low molar activity products. For instance, a recent report by Nicewicz and Li demonstrated photochemical cation radical-accelerated (CRA) substitution<sup>21</sup> as a novel mechanistic manifold for the radiofluorination of electron rich (hetero)aryl halides. However, the transformation is limited to arenes with a relatively narrow range of redox potentials; furthermore, it works best with aryl fluoride precursors, which then afford low molar activity products. Our team recently reported several complementary Cu-mediated methods for the direct radiofluorination of aryl halides; however, these are limited by the requirement for high energy UV irradiation<sup>22</sup> and/or the installation of directing groups proximal to the  $\text{C}(\text{sp}^2)\text{-X}$  bond.<sup>23</sup>

We demonstrate herein the development of a versatile radiofluorination of (hetero)aryl halides (halide = Cl, Br, I) involving sequential Pd-catalysed Miyaura borylation/Cu-mediated radiofluorination (Scheme 1). This method is highly reproducible and exhibits broad substrate scope and functional group compatibility. Furthermore, it proceeds in high radiochemical yield even when the initial borylation yield is modest. This sequence is showcased in the radiofluorination of bioactive molecules including a series of amino acids and peptides. Note: since radioactivity is hazardous, work was conducted by trained personnel in a dedicated radiochemistry facility, according to all institutional, state and federal rules, and the As Low As Reasonably Achievable (ALARA) principles.

## Results and discussion

The first step of the proposed sequence involves the selective borylation of a  $\text{C}(\text{sp}^2)\text{-halogen}$  bond. We targeted Pd-catalysed Miyaura borylation, since it is well-documented to proceed with high functional group tolerance under mild conditions and low catalyst loading.<sup>24</sup> Using 4-iodobiphenyl as a test substrate, Miyaura borylation was performed under literature conditions (1 mol% of  $\text{Pd}(\text{OAc})_2$ , 3 mol% of XPhos, 1.2 equiv. of  $\text{B}_2\text{Pin}_2$ , 2.2 equiv. of potassium 2-ethyl hexanoate (KEH) in isopropyl acetate).<sup>25,26</sup> The crude mixture was then telescoped directly to Cu-mediated radiofluorination (using  $\text{Cu}(\text{OTf})_2$ , pyridine, and 51.4 MBq (1.39 mCi)  $\text{K}^{18}\text{F}$  in DMA/*n*-BuOH). However, this sequence failed to afford any of the radiofluorinated product **2a** (Scheme 2A).



Scheme 2 (A) Attempt at tandem Miyaura borylation/CMRF with potassium 2-ethylhexanoate (KEH). (B) Additive effects show that KEH and KI inhibit CMRF. (C) Attempt at tandem Miyaura borylation/CMRF with  $\text{K}_3\text{PO}_4$ .

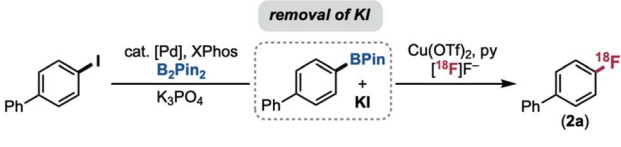
Analysis following the first step revealed that the borylated intermediate **1a** was formed in 96% yield (Scheme 2A). Furthermore, an isolated sample of **1a** underwent radiofluorination in 97% radiochemical yield (RCY, calculated using a combination of radio-TLC (for yield of organic and inorganic  $^{18}\text{F}$ ) and radio-HPLC (for purity of organic  $^{18}\text{F}$  products) as detailed on p. S32 of the SI). These results indicate that some component(s) carried over from the borylation reaction impedes the radiofluorination step. To diagnose the problem, the CMRF of **1a** was conducted in the presence of each of the borylation reagents (added in the maximum concentration that could be carried forward from the first step). As shown in Scheme 2B,  $\text{Pd}(\text{OAc})_2$ , XPhos, and  $\text{B}_2\text{Pin}_2$  led to modest decreases in the yield of **2a**. In contrast, KEH completely inhibited CMRF, suggesting that this salt is the problematic component. We hypothesize that KEH reacts with  $\text{Cu}(\text{OTf})_2$  to form the carboxylate complex  $\text{Cu}(\text{KEH})_2$ . Control studies reveal that analogous  $\text{Cu}(\text{II})$  carboxylates (*e.g.*,  $\text{Cu}(\text{OAc})_2$ ) do not mediate CMRF (see SI, p. S28).

While carboxylates are the most common bases used in Miyaura borylation, several reports have shown that phosphate salts are also effective.<sup>25</sup> Encouragingly, additive studies revealed that  $\text{K}_3\text{PO}_4$  is compatible with the CMRF step (Scheme 2B). Furthermore,  $\text{Pd}(\text{OAc})_2/\text{XPhos}$ -catalysed borylation with  $\text{K}_3\text{PO}_4$  gives 57% yield of the borylated product **1a**. However, the sequential borylation/CMRF with  $\text{K}_3\text{PO}_4$  still failed to afford any of the  $^{18}\text{F}$ -labelled product **2a** (Scheme 2C).

We next reasoned that KI, a by-product of the borylation step, was likely impeding radiofluorination. The negative impact of KI was confirmed by additive studies, with <1% RCY of **2a** obtained for CMRF in the presence of 1 equiv. of KI (Scheme 2B). To remove this byproduct, we first explored filtration of the crude borylation mixture using sorbents that are expected to retain the salt. Using either a quaternary methyl ammonium (QMA) ion exchange resin (Table 1, entry 2) or a silica gel filter (entry 3) led to complete recovery of radiofluorination reactivity



Table 1 Optimization of Pd-catalysed borylation-CMRF of 4-iodobiphenyl



Entry	Removal of KI	Yield 2a (%)
1	None; directly sample crude mixture	<1
2	QMA filter	92 ± 2
3	Silica gel filter	91 ± 1
4	Nylon syringe filter	86 ± 6
5	Allow precipitates to settle; transfer solution	85 ± 9

(>90% RCY) and high reproducibility (standard deviations of ±1–2%). Further experiments revealed that sorbent is not required in this filtration: simple mechanical filtration with a nylon syringe filter led to 86 ± 6% RCY of **2a** (entry 4) due to the low solubility of KI in the isopropyl acetate solvent. Allowing the insoluble salts to settle for ~30 min and then carefully transferring the solution phase also led to good radiochemical yield, albeit with higher variability (85 ± 9 RCY; entry 5). We ultimately moved forward with the nylon syringe filter procedure, since this proved inexpensive, simple, fast, and reproducible.

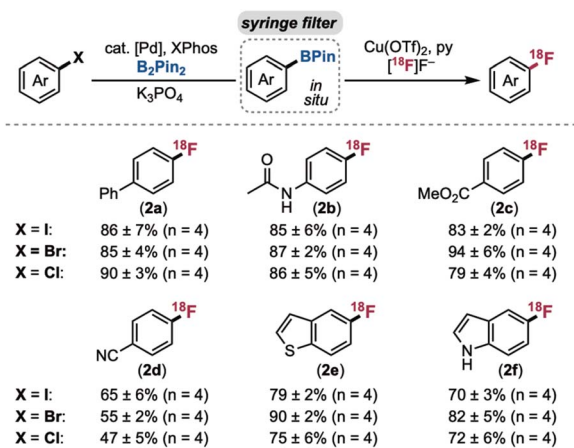
A test set of six electronically diverse (hetero)aryl iodide, -bromide, and -chloride substrates was next evaluated using the optimised procedure: (i) Pd-catalysed Miyaura borylation with K<sub>3</sub>PO<sub>4</sub>, (ii) filtration of the crude mixture through a nylon syringe filter, and (iii) Cu-mediated radiofluorination. All of the (hetero)aryl iodides and bromides afforded good to excellent radiochemical yields using commercial reagents stored and dispensed on the benchtop (Scheme 3). Minimal difference in

yield was observed upon changing from -I to -Br, and the reactions were all highly reproducible (standard deviations of ≤±7). The (hetero)aryl chlorides gave comparable yields after three modifications to the borylation conditions: (i) the Pd pre-catalyst was changed from Pd(OAc)<sub>2</sub> to Pd<sub>2</sub>(dba)<sub>3</sub>, (ii) the XPhos ligand was stored and dispensed under N<sub>2</sub> atmosphere, and (iii) the temperature was increased to 110 °C. These changes enhanced both reproducibility and yield with these less activated substrates.<sup>33</sup>

A broader set of (hetero)aryl halide derivatives was next evaluated to establish the scope and limitations of the method. As shown in Scheme 4, borylation/radiofluorination proved effective for accessing electronically diverse <sup>18</sup>F-labelled (hetero)arenes. Products bearing electron-donating alkyl, phenol, ether, and aniline substituents (**2g–2o**) are particularly noteworthy, since these are not accessible *via* traditional S<sub>N</sub>Ar radiofluorination of the aryl halide starting materials. Notably, even the 4-dimethylamino substrate, which was reported as unreactive starting from the isolated aryl boronate ester,<sup>19</sup> afforded **2jj** in 29% RCY. Various heterocycles proved compatible, including quinoline (**2t**), benzothiazole (**2u**), oxazole (**2v**), pyridine (**2w**), and benzofuran (**2x**). Across all these substrates, the borylation/radiofluorination sequence afforded moderate to high RCC and standard deviations of <±9%.<sup>27</sup>

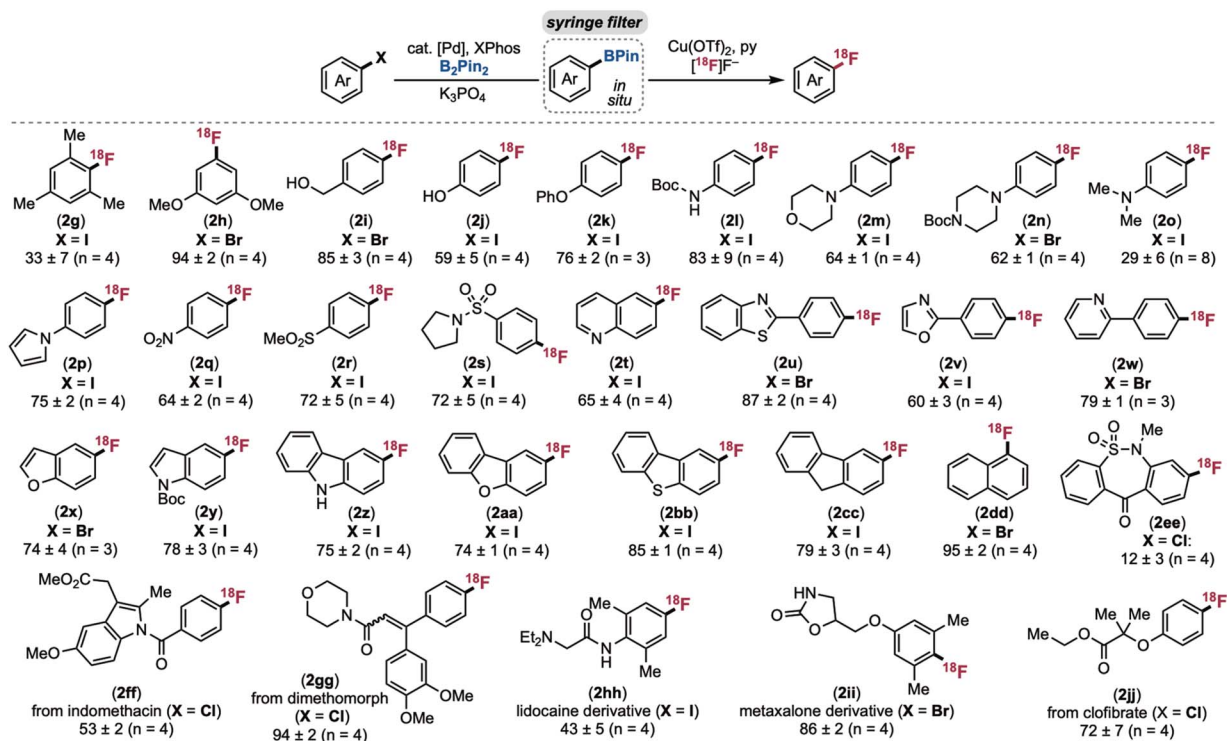
Bioactive molecules containing aryl halides, including indomethacin, dimethomorph, and clofibrate were converted to the corresponding <sup>18</sup>F derivatives (**2ff**, **2gg**, and **2jj**) in good to excellent radiochemical yields. Products **2ff** and **2gg** are the first <sup>18</sup>F-analogues of these scaffolds. For **2jj**, the radiochemical yield (72 ± 7%) was significantly higher than the 40 ± 3% RCY obtained using Nicewicz and Li's photochemical CRA approach.<sup>21</sup> Notably, with dimethomorph, the borylation step proceeded in just 35% yield. Despite this, the radiofluorinated product **2gg** was obtained in excellent radiochemical yield (94 ± 2%). This result highlights a key advantage of this method – high borylation yield is not required to obtain high radiochemical yield due to the change of limiting reagent between the two steps (from (hetero)aryl halide in step 1 to K<sup>18</sup>F in step 2). An <sup>18</sup>F-labelled analogue of metaxalone (**2ii**) was also prepared in 86 ± 2% RCY using this method, demonstrating compatibility with a sterically hindered aryl bromide substrate.

Many of these <sup>18</sup>F-labelled bioactive molecules are challenging to access from aryl halides using literature methods. For instance, nucleophilic aromatic substitution<sup>28</sup> is not viable for the radiofluorination of electron-rich/neutral aryl halides to form **2gg**, **2hh**, **2ii**, and **2jj** (or the <sup>18</sup>F-amino acids and peptides in Scheme 5; *vide infra*). Nicewicz and Li's CRA-S<sub>N</sub>Ar radiofluorination would likely struggle to generate **2ff**, **2gg**, or many of the amino acids/peptides in Scheme 5 due to the redox potentials of the halide-containing rings.<sup>21</sup> Our (NHC)Cu (NHC = N-heterocyclic carbene)-mediated radiofluorination<sup>23</sup> only works with pyridine or imine directing groups proximal to the C(sp<sup>2</sup>)-halogen bond, a feature that is not present in any of these substrates. Finally, our UV light-promoted Cu-mediated radiofluorination affords modest yield and functional group compatibility even with simple substrates.<sup>22</sup>

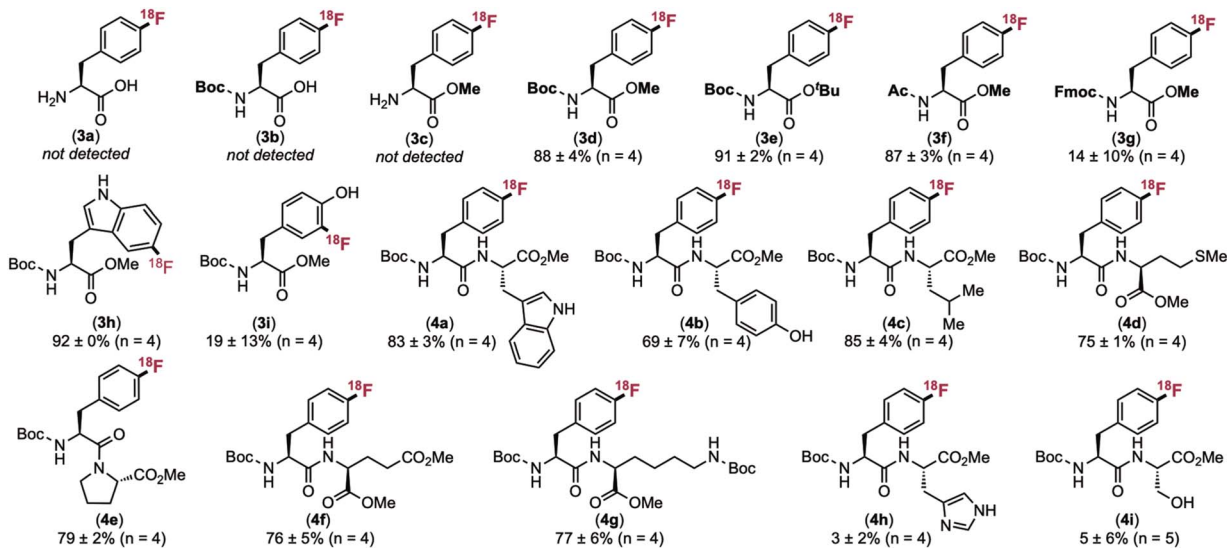


Scheme 3 Comparison of (hetero)aryl halides. Borylation conditions: <sup>a</sup>ArI/ArBr: 1 mol% of Pd(OAc)<sub>2</sub>, 3 mol% of XPhos, 2 equiv. of B<sub>2</sub>Pin<sub>2</sub>, 3 equiv. of K<sub>3</sub>PO<sub>4</sub> in isopropyl acetate at 85 °C. <sup>b</sup>ArCl: 4 mol% of Pd<sub>2</sub>(dba)<sub>3</sub>, 8 mol% of XPhos, 3 equiv. of B<sub>2</sub>Pin<sub>2</sub>, 3 equiv. of K<sub>3</sub>PO<sub>4</sub> in isopropyl acetate at 110 °C.





Scheme 4 Scope of the tandem Pd-catalysed borylation/CMRF (data represents RCYs).



Scheme 5 Amino acid and peptide substrates.

The bioactive substrates in Schemes 4 and 5 also illustrate the advantages of this new approach compared to our prior tandem C–H borylation/CMRF method.<sup>20</sup> For instance,  $^{18}\text{F}$ -lidocaine derivative **2hh** was accessed in  $43 \pm 5\%$  RCY yield using the current method *versus* just  $15 \pm 8\%$  RCY *via* C–H borylation/CMRF.  $^{18}\text{F}$ -Phenylalanine derivative **3a** (Scheme 5) was obtained in  $88 \pm 4\%$  RCY yield as a single isomer from the corresponding aryl iodide. In contrast, C–H borylation/CMRF afforded a 1 : 1.7 mixture regioisomers in  $51 \pm 17\%$  RCY yield.

Finally, products like **2ii** are not accessible *via* the sterically-controlled C–H borylation approach due the high degree of congestion at the labelling site.

A final set of studies focused in applying this sequence to the  $^{18}\text{F}$ -labelling of amino acid and peptide substrates. As peptide-based therapeutics emerge at an accelerating pace,<sup>29</sup> there is high demand for radiolabelled analogues to study bi-odistribution, quantify target engagement, and conduct *in vivo* disease diagnosis and treatment.<sup>30</sup> Most current approaches to



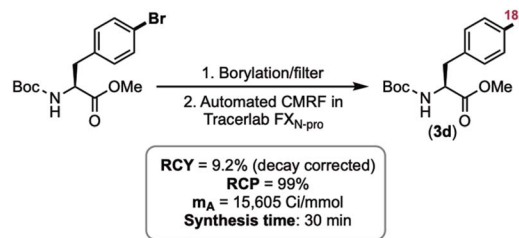
peptide radiofluorination utilize large  $^{18}\text{F}$ -containing prosthetic groups.<sup>31</sup> While these enable late-stage radiolabelling and generate readily separable products, prosthetics can alter target affinity and physicochemical properties. As such, strategies for the direct  $^{18}\text{F}$ -radiolabelling of peptides with minimal structural perturbation (*e.g.* converting phenylalanine to [ $^{18}\text{F}$ ]fluorophenylalanine) are in high demand.<sup>32</sup>

We first sought to identify protecting group schemes compatible with the borylation/CMRF of 4-iodophenylalanine derivatives. Unprotected, N-Boc protected, and C-methyl protected 4-iodo-L-phenylalanine afforded none of the corresponding radiofluorinated products **3a–c**. Control studies revealed that both the borylation and CMRF steps proceed in <10% yield with these substrates. However, protection of the C- and N-termini with Me and Boc, respectively, led to excellent ( $88 \pm 4\%$ ) radiochemical yield of **3d**. N-Acyl and C-*tert*-butyl protecting groups also proved compatible (**3e** and **3f**). In contrast, N-Fmoc led to large drop in both yield and reproducibility of the borylation/radiofluorination sequence ( $14 \pm 10\%$  RCY of **3g**). Here, the borylation step leads to competing deprotection of the Fmoc group, likely due to the basic conditions. Boc-5-Br-L-Trp-OMe was also a viable substrate, yielding  $83 \pm 3\%$  RCY of **3h**. This is another example where a high RCY is obtained despite a low (25%) yield in the borylation step.

We next explored a series of dipeptides containing an N-terminal Boc-4-iodo-L-phenylalanine to assess compatibility with common side chain functional groups. Various C-terminal amino acids with unprotected side chains, including tryptophan, tyrosine, and methionine, were well tolerated (see products **4a**, **4b**, and **4d**). However, modest radiochemical conversion ( $\leq 5\%$ ) was obtained for the C-terminal histidine and serine products **4h** and **4i**, indicating that protection of some side chain functional groups will be required in application of this method to more complex peptides.

Finally, we pursued the automation of this method on a TracerLab FX<sub>N-pro</sub> synthesis module. Translation of new radiochemistry methods to automated synthesis is crucial for accessing clinical doses of radiotracers, which typically require at least 20 mCi of activity at end-of-synthesis to allow for a 10 mCi injection after completion of QC testing and transport to the PET imaging suite. The manual reactions in Schemes 4 and 5 were performed using  $\sim 51.4$  MBq (1.39 mCi) of starting  $^{18}\text{F}$  per vial, while a typical automated run uses 66.6 GBq ( $\sim 1.8$  Ci) of activity. Protected bromophenylalanine was used as a test case for automation. The borylation step and filtration were conducted manually, and then the crude mixture was loaded into the TracerLab FX<sub>N-pro</sub> synthesis module for Cu-mediated radiofluorination. Following semi-preparative HPLC purification, product **3d** was obtained in a 9.2% decay-corrected radiochemical yield (RCY), 99% radiochemical purity (RCP), and a molar activity of 578 TBq mmol<sup>-1</sup> (15 605 Ci mmol<sup>-1</sup>  $n = 2$ ). Importantly the bromo precursor, borylated intermediate, and radiofluorinated product exhibit baseline separation by HPLC (pp. S100–S102), enabling facile purification of the target product **3d**.

The automated radiochemical yield (9.2%) is significantly lower than the manual yield (88%) for this substrate. However, automated synthesis starting from the isolated BPin precursor



Scheme 6 Automated synthesis of **3d**.

afforded **3d** in comparable (13%) radiochemical yield, demonstrating that this drop in yield between manual and automated radiosynthesis is a general feature of CMRF rather than the telescoped sequence.<sup>34</sup> In general, automated yields are well-precedented to be significantly lower than those for manual reactions for several reasons. First automation involves multiple steps and transfers of material, while the manual reactions are performed in a single step in a single vessel. Second, manual reactions start from soluble fluoride, with yields calculated relative to the fluoride added to the reaction mixture. In contrast, automated yields are calculated based on the total isolated product (non-decay-corrected) and starting amount of fluoride delivered from the cyclotron. Despite a lower automated yield compared to the manual test reactions, this automated sequence nevertheless delivers >5.5 GBq (>150 mCi) total activity of **3d**. This is sufficient for both preclinical evaluation and several human doses of this material from a single production batch, demonstrating the feasibility of applying the sequential borylation/radiofluorination sequence to PET radiotracer synthesis in a (pre)clinical setting (Scheme 6).

## Conclusions

In conclusion, this report showcases a tandem borylation-radiofluorination reaction of (hetero)aryl halides that provides access to a wide variety of  $^{18}\text{F}$ -labelled molecules. The (hetero)aryl halide (halide = Cl, Br or I) are readily available, inexpensive, and stable, and numerous functionalized derivatives (including bioactive molecules, amino acids, and dipeptides) are viable substrates. Key advantages of this approach include: (1) a wide substrate scope that is insensitive to the electronic and steric properties of the (hetero)aryl halide, (2) the ability to obtain high radiochemical yield even if the borylation step is inefficient, (3) the effectiveness of this transformation for (hetero)aryl halide substrates that are challenging to radiofluorinate using existing methods, and (4) the feasibility of high yielding radiofluorination of peptides, substrates of high interest for emerging diagnostic and therapeutic radiopharmaceuticals. These benefits widen the chemical space compatible with CMRF, enabling straightforward access to more diverse radiopharmaceuticals for PET imaging.

## Author contributions

A. N. N. developed and optimized the reaction sequence, designed and evaluated the substrate scope, and synthesized



reference standards and labelling precursors of all non-peptide substrates. S. G. G. optimized the peptide radiolabelling reactions and synthesized labelling precursors and reference standards of all peptide substrates. M. H. and T. E. S. provided critical guidance on experimental design and planning, particularly at the outset of the project. A. N. N., S. G. G., J. A. W., and A. F. B. performed radiolabelling studies. D. N. and S. G. G. performed preliminary studies on the compatibility of different protecting groups for peptides in CMRF. M. S. S. and P. J. H. S. directed all aspects of the project and secured funding. All the authors contributed to writing/editing the manuscript.

## Conflicts of interest

The authors declare no competing financial interests.

## Data availability

Further details of experimental methods, additional analysis, and analytical data, as well as supplemental figures including NMR spectra, analytical radioTLC and radioHPLC traces, and additional screening and control experiments are included in the supplementary information (SI). Supplementary information is available. See DOI: <https://doi.org/10.1039/d6sc01625a>.

## Acknowledgements

The National Institutes of Health (R01EB021155) is gratefully acknowledged for support of this work. We thank Dr Karsten Donebauer and Dr Eric Webb for helpful discussions on the sequential reaction sequence, and Dr Monica Rivas for helpful discussions on peptide synthesis and purification.

## Notes and references

- (a) W. A. Weber, J. Czernin, C. J. Anderson, R. D. Badawi, H. Barthel, F. Bengel, L. Bodei, I. Buvat, M. DiCarli, M. M. Graham, J. Grimm, K. Herrmann, L. Kostakoglu, J. S. Lewis, D. A. Mankoff, T. E. Peterson, H. Schelbert, H. Schöder, B. A. Siegel and H. W. Strauss, *J. Nucl. Med.*, 2020, **61**, 263S–272S; (b) S. Dhoundiyal, S. Srivastava, S. Kumar, G. Singh, S. Ashique, R. Pal, N. Mishra and F. Taghizadeh-Hesary, *Eur. J. Med. Res.*, 2024, **29**, 26.
- R. Halder and T. Ritter, *J. Org. Chem.*, 2021, **86**, 13873–13884.
- D. J. Donnelly, PET Imaging in Drug Discovery & Development, in *Handbook of Radiopharmaceuticals: Methodology and Applications*, ed. Scott P. J. H., and Kilbourn M., John Wiley & Sons, Chichester, 2020, pp. 703–725.
- M. Djekidel, *Front. Nucl. Med.*, 2023, **3**, 1213714.
- W. A. Weber, J. Czernin, C. J. Anderson, R. D. Badawi, H. Barthel, F. Bengel, L. Bodei, I. Buvat, M. DiCarli, M. M. Graham, J. Grimm, K. Herrmann, L. Kostakoglu, J. S. Lewis, D. A. Mankoff, T. E. Peterson, H. Schelbert, H. Schöder, B. A. Siegel and H. W. Strauss, *J. Nucl. Med.*, 2020, **61**, 263S–272S.
- (a) A. L. Vävere and P. J. H. Scott, *Semin. Nucl. Med.*, 2017, **47**, 429–453; (b) C. Mason, G. R. Gimblet, S. E. Lapi and J. S. Lewis, *Radiol. Clin. North Am.*, 2021, **59**, 887–918.
- (a) J. S. Wright, T. Kaur, S. Preshlock, S. S. Tanzey, W. P. Winton, L. S. Sharninghausen, N. Wiesner, A. F. Brooks, M. S. Sanford and P. J. H. Scott, *Clin. Transl. Imaging*, 2020, **8**, 167–206; (b) J. S. Wright, L. S. Sharninghausen, A. Lapsys, M. S. Sanford and P. J. H. Scott, *ACS Cent. Sci.*, 2024, **10**, 1674–1688; (c) G. D. Bowden, M. M. Muller, M. M. Herth, M. S. Sanford and P. J. H. Scott, *npj Imaging*, 2025, **3**, 25.
- (a) H. Sun and S. G. DiMagno, *Angew. Chem., Int. Ed.*, 2006, **45**, 2720–2725; (b) O. Jacobson, D. O. Kiesewetter and X. Chen, *Bioconjugate Chem.*, 2015, **26**, 1–18.
- N. Ichiishi, A. F. Brooks, J. J. Topczewski, M. Rodnick, M. S. Sanford and P. J. H. Scott, *Org. Lett.*, 2014, **16**, 3224–3227.
- (a) Y. Ye, S. D. Schimler, P. S. Hanley and M. S. Sanford, *J. Am. Chem. Soc.*, 2013, **135**, 16292–16295; (b) A. Mossine, A. F. Brooks, K. J. Makaravage, J. M. Miller, N. Ichiishi, M. S. Sanford and P. J. H. Scott, *Org. Lett.*, 2015, **17**, 5780–5783.
- M. Tredwell, S. M. Preshlock, N. J. Taylor, S. Gruber, M. Huiban, J. Passchier, J. Mercier, C. Génicot and V. Gouverneur, *Angew. Chem., Int. Ed.*, 2014, **53**, 7751–7755.
- (a) R. Richarz, P. Krapf, F. Zarrad, E. A. Urusova, B. Neumaier and B. D. Zlatopolskiy, *Org. Biomol. Chem.*, 2014, **12**, 8094–8099; (b) J. Zischler, N. Kolks, D. Modemann, B. Neumaier and B. D. Zlatopolskiy, *Chem. – Eur. J.*, 2017, **23**, 3251–3256.
- (a) D. Antuganov, M. Zykov, V. Timofeev, K. Timofeeva, Y. Antuganova, V. Orlovskaya, O. Fedorova and R. Krasikova, *Eur. J. Org. Chem.*, 2019, **2019**, 918–922; (b) D. Zhou, W. Chu and J. A. Katzenellenbogen, *J. Comp. Radiopharm.*, 2022, **65**, 13–20; (c) D. Zhou, W. Chu, H. Chen and J. Xu, *ACS Med. Chem. Lett.*, 2023, **15**, 116–122; (d) C. Hoffmann, N. Kolks, D. Smets, A. Haseloer, B. Gröner, E. A. Urusova, H. Endepols, F. Neumaier, U. Ruschewitz, A. Klein, B. Neumaier and B. D. Zlatopolskiy, *Chem. – Eur. J.*, 2023, **29**, e202202965; (e) J. Sun, C. Jaworski, R. Schirmacher and D. G. Hall, *Chem. – Eur. J.*, 2024, **30**, e202400906.
- (a) A. V. Mossine, S. S. Tanzey, A. F. Brooks, K. J. Makaravage, N. Ichiishi, J. M. Miller, B. D. Henderson, M. B. Skaddan, M. S. Sanford and P. J. H. Scott, *Org. Biomol. Chem.*, 2019, **17**, 8701–8705; (b) A. V. Mossine, S. S. Tanzey, A. F. Brooks, K. J. Makaravage, N. Ichiishi, J. M. Miller, B. D. Henderson, T. Erhard, C. Bruetting, M. B. Skaddan, M. S. Sanford and P. J. H. Scott, *Nat. Protoc.*, 2020, **15**, 1742–1759.
- T. Gendron, G. Destro, N. J. W. Straathof, J. B. I. Sap, F. Guibbal, C. Vriamont, C. Caygill, J. R. Atack, A. J. Watkins, C. Marshall, R. Hueting, C. Warnier, V. Gouverneur and M. Tredwell, *EJNMMI Radiopharm. Chem.*, 2022, **7**, 5.
- R. Schirmacher, J. J. Bailey, A. V. Mossine, P. J. H. Scott, L. Kaiser, P. Bartenstein, S. Lidner, D. R. Kaplan, A. Kostikov, G. Fricker, A. Mahringer, P. Rosa-Neto,



- E. Schirmmacher, C. Wängler, B. Wängler, A. Thiel, J. P. Soucy, V. Bernard-Gauthier, *et al.*, *J. Med. Chem.*, 2018, **61**, 1737–1743.
- 17 (a) F. W. Friese and A. Studer, *Chem. Sci.*, 2019, **10**, 8503–8518; (b) M. Wang and Z. Shi, *Chem. Rev.*, 2020, **120**, 7348–7398; (c) Z.-H. Shang, J. Pan, Z. Wang, Z.-X. Zhang and J. Wu, *Eur. J. Org. Chem.*, 2023, **26**, e202201379; (d) J. S. Wright, P. J. H. Scott and P. G. Steel, *Angew. Chem., Int. Ed.*, 2020, **60**, 2796–2821.
- 18 T. Kaur, X. Shao, M. Horikawa, L. S. Sharninghausen, S. Preshlock, A. F. Brooks, B. D. Henderson, R. A. Koeppe, A. F. DaSilva, M. S. Sanford and P. J. H. Scott, *Org. Process Res. Dev.*, 2023, **27**, 373–381.
- 19 N. Hadjipaschalis, S. Ortalli, Z. Chen, R. S. Paton, J. Ford, M. Tredwell and V. Gouverneur, *Org. Lett.*, 2025, **27**, 6545–6550.
- 20 J. S. Wright, L. S. Sharninghausen, S. Preshlock, A. F. Brooks, M. S. Sanford and P. J. H. Scott, *J. Am. Chem. Soc.*, 2021, **143**, 6915–6921.
- 21 W. Chen, H. Wang, N. E. S. Tay, V. Pistritto, K.-P. Li, T. Zhang, Z. Wu, D. A. Nicewicz and Z. Li, *Nat. Chem.*, 2022, **14**, 216–223.
- 22 T. E. Spiller, K. Donabauer, A. F. Brooks, J. A. Witek, G. D. Bowden, P. J. H. Scott and M. S. Sanford, *Org. Lett.*, 2024, **36**, 6433–6437.
- 23 L. S. Sharninghausen, A. F. Brooks, W. P. Winton, K. J. Makaravage, P. J. H. Scott and M. S. Sanford, *J. Am. Chem. Soc.*, 2020, **142**, 7362–7367.
- 24 W. K. Chow, O. Y. Yuen, C. M. So, C. P. Lau, W. T. Wong and F. Y. Kwong, *RSC Adv.*, 2012, **3**, 12581–12539.
- 25 S. Barroso, M. Joksich, P. Puylaert, S. Tin, S. J. Bell, L. Donnellan, S. Duguid, C. Muir, P. Zhao, V. Farina, D. N. Tran and J. G. de Vries, *J. Org. Chem.*, 2021, **86**, 103–109.
- 26 T. Ishiyama, M. Murata and N. Miyaura, *J. Org. Chem.*, 1995, **60**, 7508–7510.
- 27 Unsuccessful substrates (giving <1% radiochemical yield) are summarized in SI page 25. In most cases, these are also unsuccessful starting from the pure Ar-BPin, indicating that the CMRF step is the problem.
- 28 S. J. Lee, M. T. Morales-Colón, A. F. Brooks, J. S. Wright, K. J. Makaravage, P. J. H. Scott and M. S. Sanford, *J. Org. Chem.*, 2021, **86**, 14121–14130.
- 29 (a) L. Wang, N. Wang, W. Zhang, X. Cheng, Z. Yan, G. Shao, X. Wang, R. Wang and C. Fu, *Signal Transduct. Targeted Ther.*, 2022, **7**, 48; (b) L. Costa, E. Sousa and C. Fernandes, *Pharmaceuticals*, 2023, **16**, 996; (c) X. Ji, A. L. Nielsen and C. Heinis, *Angew. Chem. Int. Ed. Engl.*, 2024, **63**, e202308251.
- 30 (a) S. Richter and F. Wuest, *Molecules*, 2014, **19**, 20536–20556; (b) I. M. Jackson, P. J. H. Scott and S. Thompson, *Semin. Nucl. Med.*, 2017, **47**, 493–523; (c) G. P. Nicolas, A. Morgenstern, M. Schottelius and M. Fani, *J. Nucl. Med.*, 2019, **60**, 167–171; (d) A. J. Hall and M. B. Haskali, *Aust. J. Chem.*, 2022, **75**, 34–54.
- 31 (a) D. Van der Born, A. Pees, A. J. Poot, R. V. A. Orru, A. D. Windhorst and D. Vugts, *Chem. Soc. Rev.*, 2017, **46**, 4709–4773; (b) O. Morris, O. M. Fairclough, J. Grigg, C. Prenant and A. McMahon, *J. Labelled Compd. Radiopharm.*, 2019, **62**, 4–23; (c) C. Rangger and R. Haubner, *Pharmaceuticals*, 2020, **13**, 22.
- 32 (a) J. Rickmeier and T. Ritter, *Angew. Chem., Int. Ed.*, 2018, **57**, 14207–14211; (b) R. Halder, G. Ma, J. Rickmeier, J. W. McDaniel, R. Petzold, C. N. Neumann, J. M. Murphy and T. Ritter, *Nat. Protoc.*, 2023, **18**, 3614–3651.
- 33 K. Billingsley, T. E. Barder and S. L. Buchwald, *Angew. Chem., Int. Ed.*, 2007, **46**, 5359–5363.
- 34 The radiochemical yield for the automation is within the expected range for current standards for CMRF. (a) F. Guibbal, P. G. Isenegger, T. C. Wilson, A. Pacelli, D. Mahaut, J. B. I. Sap, N. J. Taylor, S. Verhoog, S. Preshlock, R. Hueting, B. Cornelissen and V. Gouverneur, *Nat. Protoc.*, 2020, **15**, 1525–1541; (b) A. V. Mossine, A. F. Brooks, V. Bernard-Gauthier, J. J. Bailey, N. Ichiishi, R. Schirmmacher, M. S. Sanford and P. J. H. Scott, *J. Labelled Compd. Radiopharm.*, 2018, **61**, 228–236; (c) J. S. Wright, L. S. Sharninghausen, S. Preshlock, A. F. Brooks, M. S. Sanford and P. J. H. Scott, *J. Am. Chem. Soc.*, 2021, **143**, 6915–6921; (d) M. A. Nadporojkii, V. V. Orlovskaya, O. S. Fedorova, D. S. Sysoev and R. N. Krasikova, *Molecules*, 2024, **29**, 3342; (e) K. J. Makaravage, A. F. Brooks, A. V. Mossine, M. S. Sanford and P. J. H. Scott, *Org. Lett.*, 2016, **18**, 5440–5443; (f) S. J. Lee, M. T. Morales-Colon, A. F. Brooks, J. S. Wright, K. J. Makaravage, P. J. H. Scott and M. S. Sanford, *J. Org. Chem.*, 2021, **86**, 14121–14130; (g) A. V. Mossine, S. S. Tanzey, A. F. Brooks, K. J. Makaravage, N. Ichiishi, J. M. Miller, B. D. Henderson, M. B. Skaddan, M. S. Sanford and P. J. H. Scott, *Org. Biomol. Chem.*, 2019, **17**, 8701–8705.

